A Pilot Reanalysis Project at COLA

D. A. Paolino, Q. Yang, B. Doty,
J. L. Kinter III, J. Shukla,
and David M. Straus
Center for Ocean–Land–Atmosphere Studies,
Institute of Global Environment and Society,
Calverton, Maryland

Abstract

Results are presented from a retrospective analysis of 19 months (May 1982–November 1983) of global atmospheric observations. The National Meteorological Center Global Data Assimilation System was used in tandem with the atmospheric general circulation model of the Center for Ocean–Land–Atmosphere Studies to produce four-times-daily representations of the global atmosphere. Statistics were compiled regarding the use of data by the analysis and the decisions of the quality control procedures. Comparison of the reanalyses with both observation and the archived contemporaneous analyses showed substantial improvements in the representation of the global atmospheric circulation, possibly excepting the Southern Hemisphere south of 60°S. A list of data products from the reanalysis is given in an appendix.

1. Introduction

The rapid progress in global atmospheric modeling and atmospheric observing systems since the 1960s has made possible reasonably skillful global numerical weather predictions extending to lead times of several days. Modeling has improved dramatically as a result of continual enhancements of our understanding of large-scale dynamics in both the Tropics and the extratropics, and with the ever-increasing capability of supercomputing technology. The observing system was significantly improved during the First GARP (Global Atmospheric Research Program) Global Experiment in 1979, although it has been difficult to maintain at a fairly steady level since that time. A necessary part of the numerical weather prediction process is the construction of global gridded analyses of atmospheric observations using data assimilation methods, which have also progressed significantly over the last few decades. Improvements in the statistical techniques used to merge atmospheric model output and observational data and in the quality control procedures have made it possible to consider using these by-products of numerical weather prediction efforts as surrogates for measurements of the four-dimensional structure of the global atmosphere.

Unfortunately, the steady improvement in numerical models, the incremental improvement in data assimilation techniques, and the jump in observing system capability in 1979 have made it difficult to use global gridded analyses produced for operational weather prediction as climate datasets. The changes in statistical interpolation schemes, quality control procedures, numerical weather prediction model resolution, initialization, and sub-grid-scale physical parameterization, which have been implemented over time, have introduced significant changes in the global gridded analyses (Trenberth and Olson 1988a). These variations in the record of global gridded analyses make it untenable to use these datasets for analysis of climatic time series.

Operational analyses also suffer from a time constraint imposed by the necessity to produce forecasts in real time. Since there is a limited amount of time available between the moment an observation is made and the time a forecast must be issued, there is a cutoff time beyond which observational data received over the Global Telecommunication System are not used. These so-called delayed mode data are frequently observations made in remote locations where there are few stations and therefore where those observations can make substantial contributions to the available dataset. Although these observations have been archived, they have not been used in the production of global gridded analyses, so their value has not been realized.

Bengtsson and Shukla (1988) suggested that if a single data assimilation system and a single global atmospheric model were used to process the entire time series of atmospheric observations, the problems of the inhomogeneities of the data processing system over time would be obviated. Also, all the available observational data could be collected from the various archives where they are stored, including the delayed mode data.

In addition to the global gridded analyses, other valuable data could be archived, such as the numerical

Corresponding author address: D. A. Paolino, COLA, Suite 302, 4041 Powder Mill Rd., Calverton, MD 20705
E-mail: paolino@cola.iges.org
In final form 2 December 1994.
©1995 American Meteorological Society

weather prediction model diagnostics, including three-dimensional heating, the surface flux fields, and precipitation, and also the data assimilation quality control statistics, which provide information about the fidelity of the analyses to the original observations as well as information about the quality of the observations themselves. These quality control statistics would provide a gauge on the reliability of the retrospective analyses and would aid the preprocessing of the observational data for future attempts at retrospective analysis.

The whole concept of retrospective analysis was reviewed by an ad hoc panel to determine the efficacy of such analyses for improving our understanding of global interannual climate variability (Kinter and Shukla 1989). In response, the Center for Ocean–Land–Atmosphere Studies (COLA) embarked on a feasibility study to determine whether or not a retrospective analysis of a long time series of atmospheric observations would be possible, to conduct such a reanalysis, and to determine the critical issues in conducting such a reanalysis. We selected the period 1 May 1982 to 30 November 1983 as a period in which there was a significant El Niño–Southern Oscillation event. That period predates the time when the U.S. National Meteorological Center (NMC) and the European Centre for Medium-Range Weather Forecasts (ECMWF) made substantial improvements in their data assimilation systems and numerical weather prediction models, and was also a period during which major changes were implemented in the NMC and ECMWF systems (Trenberth and Olson 1988a).

Since commencing our effort, other groups have announced plans to produce reanalyses of the global atmospheric circulation. The Data Assimilation Office at the National Aeronautics and Space Administration Goddard Space Flight Center is performing a reanalysis forward in time, starting from 1985. Model resolution is 2.5° longitude by 2.0° latitude, with 20 sigma levels (Schubert et al. 1993). NMC is undertaking a reanalysis for 1958–1993 using a T62 forecast model with 29 sigma levels, along with the spectral statistical interpolation analysis (Kalnay et al. 1993). ECMWF will reanalyze the period 1979–1992 using a T106 model with 31 vertical levels, with a new three-dimensional variational analysis (Burridge 1994). The Naval Research Laboratory is also performing a reanalysis.

The COLA reanalysis was performed using an intermittent, multivariate optimum interpolation cycle based on the Global Data Assimilation System of NMC (Dey and Morone 1985). The assimilation merges observational data with a 6-h forecast (the "first guess") produced by a numerical model of the global atmosphere. We used the COLA general circulation model (GCM) to produce the first guess (Kinter et al. 1988; Sato et al. 1989).

In the following section, the COLA reanalysis is described. The sources of data that were used are documented in section 2. The analysis procedure itself, including the implementation of complex quality control, is discussed in section 3. Section 4 provides an overview of the results of the COLA reanalysis including a discussion of the observational data that were rejected by the analysis, comparisons of the mean climate computed from operational analyses and from reanalyzed fields, and a description of the improved divergent flow in the reanalyses. A summary of the COLA reanalysis and a discussion of further issues to be resolved is provided in section 5. A listing of available COLA reanalysis products is given in the appendix.

A thorough review of the COLA reanalysis is beyond the scope of a single article. Subsequent papers will provide a more comprehensive examination of all components of the COLA reanalysis.

2. Data

a. Observations

Five data streams were used as input to the analysis: station upper-air soundings (radiosondes/rawinsondes/pilot balloons), aircraft wind reports, satellite cloud-tracked winds, ship surface pressure and winds, and TIROS (Television Infrared Observation Satellite) operational vertical soundings (TOVS). The first three datasets (Jenne 1975) were archived at the National Center for Atmospheric Research (NCAR). They are the data used in the contemporaneous NMC analyses of 1982 and 1983. The ship reports were taken from the Comprehensive Ocean–Atmosphere Data Set (COADS) (Slutz et al. 1985). About twice as many ship reports were available in the COADS data as compared with the archived ship data used in the NMC analyses of 1982 and 1983. TOVS soundings were obtained from the National Climatic Data Center (NCDC) in the form of layer mean temperatures (Kidwell 1991).

Tables 1a and 1b show various statistics for each of the data streams available to the COLA reanalysis. Separate statistics were compiled for 0000 and 1200 UTC analyses, and for 0600 and 1800 UTC analyses. Means and standard deviations (in time) of the number of observations input to the analysis were computed for all analyses with data available for each particular data type. The number of analyses with missing data is given in column five. The statistics in Tables 1a and 1b are based on 579 days of four-times-daily reanalyses.

The significant differences for data available at 0600 and 1800 UTC versus that available at 0000 and 1200 UTC were fewer station soundings of height and

wind, and fewer satellite cloud-tracked wind reports at 1800 UTC.

During some periods, data that were normally present appeared to be missing from the archive. During the period 20 April–11 May 1983, only 3 of 46 0600 and 1800 UTC data had station upper-air soundings archived. TOVS sounding product data were not available for the weeks of 22–29 May and 5–11 June 1983.

The operational analyses from NMC and ECMWF for 1982 and 1983 were obtained from the data archive at NCAR (Jenne 1975). Significant changes were made to operational models and analyses at both of these centers during the period of the COLA reanalysis. At the start of this period, NMC was using a univariate analysis of geopotential height and relative humidity, and a multivariate analysis of the zonal and meridional wind components. The model resolution was R24, with 12 sigma levels. On 14 August 1982, the model resolution was changed to R30 and the analysis became multivariate in heights and winds. NMC used an adiabatic nonlinear normal mode initialization (NNMI) at this time. ECMWF initially was using a 15-level gridpoint GCM (1.875° resolution). On 21 April 1983, the model was changed to a 16-level spectral GCM with T63 resolution. The ECMWF analysis was multivariate in geopotential height, thickness, and wind, and univariate in humidity. ECMWF used an adiabatic NNMI until 21 September 1982, when they switched to a diabatic NNMI (Trenberth and Olson 1988a; Trenberth 1992). The models at both centers predate later versions with major improvements in model physics and surface parameterizations similar to those that were used by the GCM in the COLA reanalysis.

TABLE 1a. Statistics for the number of observations (obs.) input to the analysis at 0000 and 1200 UTC. For multilevel observations, level refers to the level with the maximum number of observations. Missing refers to the number of analyses produced with no observations from that particular data stream. Means and standard deviations are computed using only those times when data is present for the particular data stream.

Observation type	Mean no. obs.	Std dev no. obs.	Pressure level (mb)	No. analyses with missing obs.
Radiosonde Z	624.5	39.1	500	3
Radiosonde RH	613.9	37.9	700	3
Upper winds	1118.3	103.2	850	3
Dropsonde Z	2.5	3.6	500	557
Dropsonde wind	2.2	3.3	500	534
TOVS (land)	1249.8	158.9	70	51
TOVS (ocean)	1946.2	245.6	850	48
Ship surface pressure	863.0	36.9	1000	0
Ship surface wind	835.9	36.7	1000	0
Aircraft wind	175.8	28.3	250	0
Satellite wind	529.2	135.6	850	2

TABLE 1b. As in Table 1a but for 0600 and 1800 UTC analyses. Satellite wind data is never available at 0600 UTC.

Observation type	Mean no. obs.	Std dev no. obs.	Pressure level (mb)	No. analyses with missing obs.
Radiosonde Z	37.4	20.6	850	61
Radiosonde RH	37.2	20.4	850	62
Upper wind	386.0	247.4	850	54
Dropsonde Z	3.1	3.2	500	450
Dropsonde wind	2.7	2.9	500	428
TOVS (land)	1141.3	144.8	70	49
TOVS (ocean)	2091.5	269.3	850	47
Ship surface pressure	840.5	51.0	1000	0
Ship surface wind	812.7	49.3	1000	0
Aircraft wind	186.8	31.2	250	0
Satellite wind	311.8	93.2	850	15

b. Boundary conditions

Observed global sea surface temperature (Reynolds and Marsico 1993) and Northern Hemisphere snow cover (Dewey and Heim 1982) were used in the initialization of each 6-h forecast. The initialized value was computed from the monthly mean values by linear interpolation from the two appropriate monthly means. The monthly mean was considered to represent the midpoint of each month.

The COLA GCM, which includes the Simple Biosphere Model (Sellers et al. 1986; Sato et al. 1989),

forecasts snow cover. Initially we intended to use the forecast snow cover to initialize the next 6-h forecast. However, we found that the GCM tended to melt an initialized snow cover after several analysis/forecast cycles. To compensate for this, the following procedure was devised. After the first guess was produced, the forecast snow cover was compared to the observed snow cover at each of the model's Gaussian grid points. If snow cover was present at the forecast grid point, but not on the observed grid point (as defined by the two interpolated monthly means), no change was made. If snow cover was not present at the forecast grid point, but was present at the observed grid point, the forecast grid point was changed to snow covered. It is assumed that this procedure also better represents the intramonthly variability of the snow cover.

Soil wetness observations were considered too sparse and unreliable, so the model-predicted soil wetness was used to initialize each following 6-h forecast.

3. Procedure

A single analysis cycle consisted of the following steps. The station soundings were corrected at upper levels (after McInturff et al. 1979) to compensate for solar radiation effects on the radiosonde temperature sensor. All five data streams were ingested. The mass data from radiosondes over India are "tossed" (i.e., rejected due to suspected poor quality), but the wind data from the same stations were retained. Ship reports with positions on land were tossed, as were TOVS soundings that had been archived with error flags. TOVS soundings were converted from layer mean temperatures to geopotential heights on the mandatory pressure levels (1000, 850, 700, 500, 400, 300, 250, 200, 150, 100, 70, and 50 mb). The difference of each observation from the first guess was computed by interpolating the appropriate forecast field to the location of each observation. These residuals of geopotential height (Z) and the horizontal wind components (u and v) were then subjected to the complex quality control procedure (OIQC) described by Woollen (1991). This procedure consisted of an iterative, multivariate optimal interpolation that checks the vertical consistency of each observation as well as checking it against neighboring observations. Observations rejected by the OIQC were not input to the analysis program. Detailed statistics were retained regarding the decisions of the OIQC on all observations from all data streams.

The analysis was multivariate for Z, u, and v but was univariate for relative humidity (Dey and Morone 1985), and incorporated all modifications to the NMC analysis up to the time NMC switched to the T80 forecast model on 12 August 1987 (see Trenberth and Olson 1988b for details). The analysis was performed on the 12 mandatory pressure levels; the RH analysis was performed only up to 300 mb. The global analysis grid had 84 points along a latitude circle (with a lower, staggered resolution poleward of 60° latitude), and 82 points along each meridian from North Pole to South Pole. Up to 30 observations were used in the multivariate Z, u, v analysis at each grid point; up to 10 observations were used at each grid point for the relative humidity analysis.

A diabatic nonlinear normal mode initialization (Machenauer 1977), with a cutoff period of 27 502 s, was performed on the analysis before it was used to initialize the next 6-h forecast.

The COLA GCM is based on a modified version of the NMC global spectral model used for medium-range weather forecasting (see Sela 1980 for the original formulation; see Kinter et al. 1988 for the modified version). The land surface parameterization was changed to a biophysically based formulation after Sellers et al. (1986) by Sato et al. (1989) and later simplified by Xue et al. (1991). The model is the same as that presented in Xue et al. (1991) except that an interactive cloud radiation scheme was added (Hou 1990; after Slingo 1987). The GCM is truncated rhomboidally at wavenumber 40. The vertical structure of the model is represented by 18 unevenly spaced vertical levels using sigma (Phillips 1957) as the vertical coordinate. The spacing of the levels is the same as that used in the NMC medium range forecast model (NMC Development Division 1988). The GCM includes parameterizations of solar radiative heating (Lacis and Hansen 1974), terrestrial radiative cooling (Harshvardhan et al. 1987), cloud radiation interaction as previously mentioned, deep convection (after Kuo 1965), shallow convection (Tiedtke 1984), large-scale condensation with a relative humidity criterion as in Sela (1980), a turbulence closure treatment of subgrid-scale exchanges of heat, momentum, and moisture (Miyakoda and Sirutis 1977; after Mellor and Yamada 1982), and biophysically controlled interactions between the vegetated land surface and the atmosphere as previously mentioned.

The retrospective analysis was started by using the 0000 UTC 25 April 1982 NMC analysis to initialize the COLA model. The COLA model then produced a 6-h forecast, which was used as the first guess for the 0600 UTC global analysis. The adjusted snow cover, the forecast soil wetness, forecast clouds, and the observed SST fields were used along with the 0600 UTC analysis to initialize the model in order to produce a first guess valid at 1200 UTC 25 April 1982.

TABLE 2. Global toss rate for data as determined by the OIQC, May 1982 through November 1983. Number of observations refers to data input to the OIQC (kept + tossed).

Observation type	Pressure level (mb)	Toss rate (%)	No. of obs. (×1000)
Heights			
Ship (surface pressure)	1000	18.3	1973
TOVS (land)	70	6.9	2649
	50	2.6	2483
TOVS (ocean)	850	17.9	4484
	70	2.0	4213
	50	1.0	4175
Winds			
Ship	1000	2.9	1909
Aircraft	300	2.7	112
	250	2.4	420
	200	2.1	327
Satellite (cloud tracked)	850	0.3	788
	300	0.4	83
	250	0.3	92
	200	0.2	196

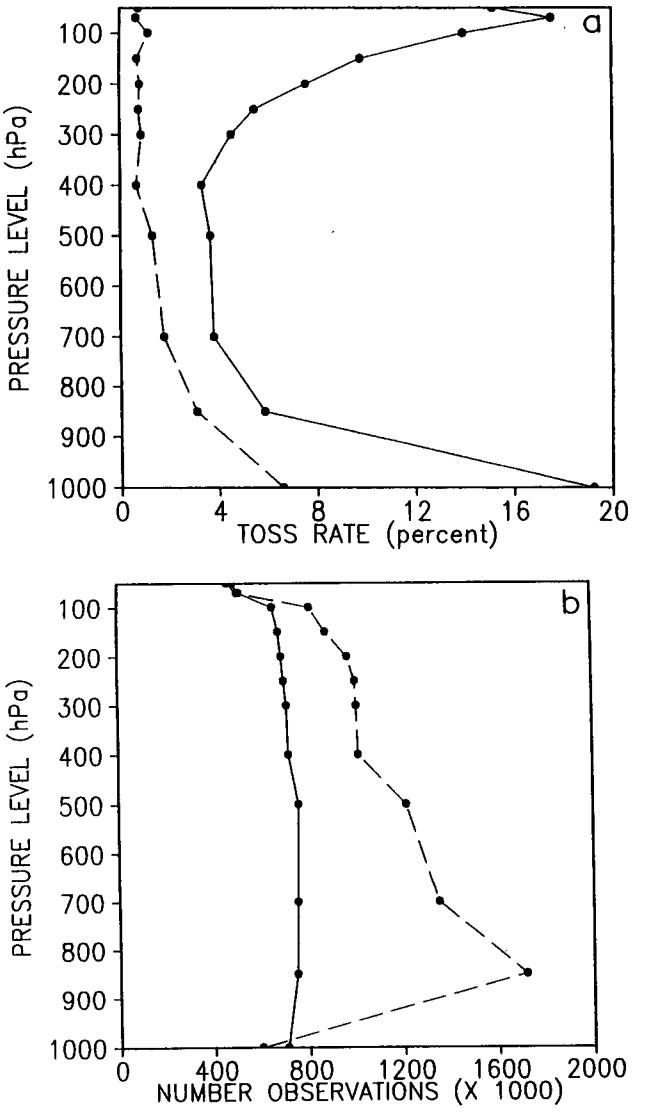

FIG. 1. (a) Toss rate (percent) for station soundings compiled for the COLA reanalysis for the period May 1982 through November 1983. The solid line represents observations of geopotential heights; the dashed line, winds. (b) Number of observations (×1000) for geopotential heights (solid line) and winds (dashed line).

The forecast/analysis cycle continued in this manner to produce the retrospective analysis.

4. Results

a. Toss rates

Global toss rates are given in Fig. 1a (for station soundings) and in Table 2 for other types of observations. The toss rate is the percentage of observations rejected by the OIQC with respect to the number of observations input to the OIQC. The values given in Fig. 1 and Table 2 represent totals for the entire period of the retrospective analysis. Statistics for wind data were compiled for layers bounded by the midpoint of the pressure levels above and below the pressure level in question. The total number of observations input to the quality control program, over the entire period of the retrospective analysis, is given in Fig. 1b and Table 2.

Observations at levels not shown in Table 2 represented 5.2% of the total observations for the aircraft winds and 7.3% of the total observations for the satellite cloud-tracked winds. Only one level is given in Table 2 for tropospheric oceanic TOVS soundings, because the OIQC tossed all levels between 850 and 100 mb, inclusive, for an oceanic TOVS sounding with at least one tossed level. In general, the OIQC tended to toss mass data at a higher rate than wind data. The high toss rate at 1000 mb for radiosondes (Fig. 1a) is partly due to stations tossed for being "below" the model surface. The toss rates for the radiosonde heights are also larger in the upper troposphere and

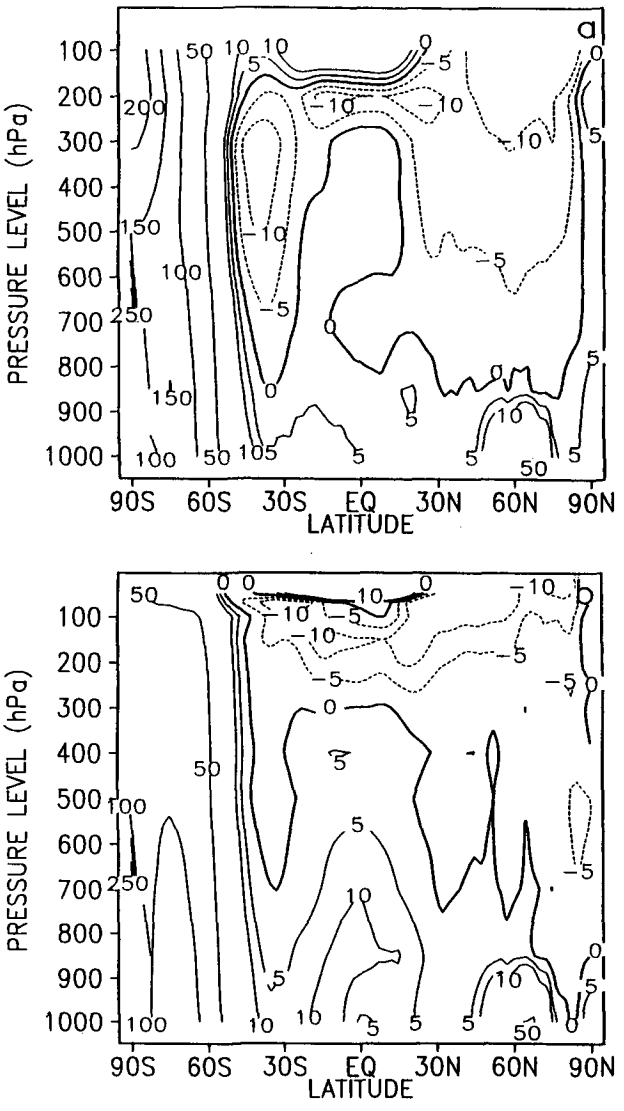

FIG. 2. Zonal mean difference of geopotential height anomalies averaged over the entire period of the COLA reanalysis. Units are meters, not uneven contour interval. (a) For the difference COLA–ECMWF. (b) For the difference COLA–NMC.

lower stratosphere. High toss rates for the oceanic TOVS in Table 2 are due mainly to high toss rates over the southern oceans in the austral winter, particularly during the winter season of JJA (June–July–August) 1983, when toss rates were more than 40% over most of the ocean south of 45°S.

b. Comparison of mean fields

Figure 2 presents the differences among the different analyses in the mean geopotential height field for the period of reanalysis: May 1982 through November 1983. Mean fields were computed on the same 2.5° by 2.5° grid for all analyses. Grid points below the surface of the COLA model are not included in the calculation of means. Results derived from the NMC and ECMWF analyses are the products of the models and analyses in operational use in 1982 and 1983.

The main feature in Fig. 2 (note irregular contour intervals) is the large difference in the mean height field over Antarctica. Seasonal mean differences are larger for the austral winter and are larger for 1983 then in 1982. Differences between the COLA analyses and the old analyses were much smaller and of opposite sign to those in Fig. 2 in the austral summer of 1982/1983. The toss rates of radiosonde heights over Antarctica were very high in the austral winter, as were the toss rates of oceanic TOVS soundings in the surrounding ocean at the same time. We speculate that these high toss rates were due in part to a drift of the model's first guess toward (erroneous) model climatology in the austral winter. The large anomalies at 1000 mb near 60°N are probably due to the treatment of surface topography in the three different analyses; most of the grid points at this latitude are below the surface of the COLA model. Large differences in the Tropics at 100 mb in Fig. 2a and at 50 mb in Fig. 2b reflect larger height values over oceans and lower values over continents for the COLA analysis.

Zonal winds in the COLA reanalysis had a less pronounced westerly component south of 30°S, when compared with the ECMWF and NMC analyses (not shown). Since the COLA analysis was multivariate in geopotential height and wind, the differences in the height analyses are reflected in the wind analyses. Maximum differences occurred near 60°S, where the vertical profile of the magnitude of the zonally averaged zonal wind for the COLA analyses is about 3–4 m s^{-1} lower throughout the troposphere, when compared to the ECMWF and NMC analyses.

Figure 3 presents mean 1000 mb virtual temperature maps for COLA, NMC, and ECMWF analyses over the tropical Pacific Ocean for the month of March 1983, along with the mean sea surface temperature field for the same month. Virtual temperature was computed from the geopotential height analyses using the identical algorithm for all three analyses. March 1983 was chosen as a month representative of the ENSO event of 1982/1983. Positive anomalies of sea surface temperature of 1°C or more extended eastward along the equator from 180° longitude almost to the coast of South America. Monthly mean virtual temperatures for the COLA (Fig. 3a) and ECMWF (Fig. 3c) analyses reflect the pattern of the underlying sea surface temperature field (Fig. 3d) fairly well. The corresponding map for the NMC analyses (Fig. 3b) seems to provide a poor representation of this ENSO event. NMC seriously underestimated the SST anomalies here during the ENSO event (Reynolds 1984), due in part to a cold bias in satellite-derived sea surface

temperatures resulting from the presence of stratospheric aerosols following the eruption of El Chichón in April 1982 (Walton 1985).

c. Root-mean-square error statistics

To measure the representativeness of the COLA retrospective analysis in comparison to the observations, root-mean-square errors (rmse) were computed between the analysis and the station upper-air soundings. The same statistics were computed for the contemporaneous NMC and ECMWF analyses, so that comparisons could be made. To produce useful statistics, it is necessary to avoid bias in the selection of stations used to compute the rmse. A bias could arise if we were to use only those stations that passed the OIQC program, since these are the exact stations used in the production of the COLA analyses. Another problem could arise if we included observations with obvious, gross errors. Most of these errors would probably have been rejected by each of the three analyses, and would artificially inflate the rmse.

Stations were chosen using the following procedure. Radiosonde stations were collected for each of the six seasons JJA 1982–SON (September–October–November) 1983. Data were collected for stations reporting at 0000 and 1200 UTC only. Height and wind data were collected only on the 12 mandatory levels. The same radiation correction used in the COLA retrospective analysis was applied to the appropriate stations. Following Gandin (1988), a hydrostatic consistency check was applied to all soundings. Any sounding that had one or more levels failing this check was discarded. Next, all soundings were subjected to a gross error check (DiMego et al. 1985) for the quantities Z and u. Data failing the gross error check were discarded. Data were subjected to an additional check to remove observations suspected of being in error and likely to have been tossed by the quality control procedures present during the production of the operational analyses. In this check, each observation was compared to each of the three analyses (COLA, NMC, ECMWF) and was discarded if it departed from any of the three analyses by more than 500 m for heights, and 50 m s^{-1} for zonal winds.

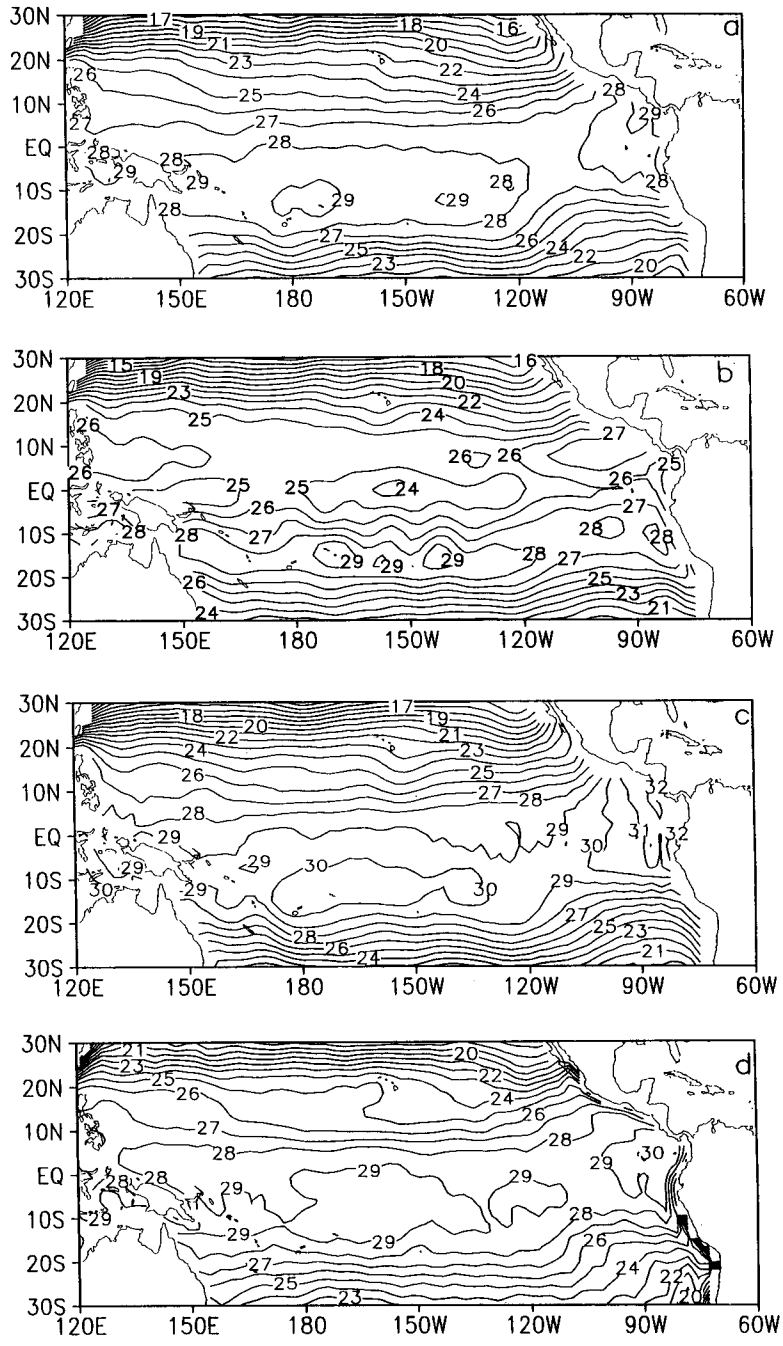

FIG. 3. (a) March 1983 monthly mean 1000-mb virtual temperature (°C) for the COLA analysis. Computed from twice daily geopotential height analyses. (b) As in Fig. 3a but for the NMC analysis. (c) As in Fig. 3a but for the ECMWF analysis. (d) March 1983 monthly mean sea surface temperature (°C).

Stations with fewer than 60 soundings (40 soundings between 20°S and 20°N) in an individual season were discarded for that season. We refer to this dataset as the "thinned radiosonde."

The stations that passed the above checks may still contain observation errors, systematic errors, and errors due to nonrepresentativeness (see, for ex-

ample, Gandin 1988). We assume that the observation errors will be random in time and space. We made no investigation for systematic errors, although we did not use the height profiles for stations in India in the calculation of the rmse. The NMC and ECMWF analyses of 1982 and 1983 may have used many of these stations. We consider the OIQC to be superior to the methods used for quality control at the time of the contemporaneous analyses. The nonrepresentative errors present in the thinned radiosondes were more likely to have been accepted in the contemporaneous analyses and rejected by the OIQC in the COLA analyses. We then consider these rmse to be biased against the COLA analysis, except where the NMC and ECMWF may have used the mass data in the Indian radiosondes.

Root-mean-square error statistics were computed between the thinned radiosondes and the analyses, for Z and u on the mandatory levels, using all 0000 and 1200 UTC analyses. The value of the analysis at the location of the station was computed by a linear interpolation of the four surrounding analysis grid points. There are no missing COLA or ECMWF analyses. Root-mean-square error statistics for the NMC analyses were computed from a smaller number of analyses. For the period for which the rmse statistics are computed, 172 out of a possible 1096 (15.7%) of the NMC analyses are missing.

Tables 3 and 4 display the rmse statistics accumulated over 30° latitude bands, for the geopotential height and zonal wind analyses of COLA and ECMWF for June 1982–November 1983. Root-mean-square errors for the NMC analyses are described but not shown here. Large values of the rmse might suggest some systematic error in the model/analysis system or with the radiosonde data itself. Smaller differences in the rmse computed for the different analyses are more difficult to interpret, but we believe that when the data are averaged over as large an area and for as long a time period as we have done, lower values of rmse should at least indicate that a good analysis has been produced. Table 3 shows that the rmse south of 30°S is significantly larger for the COLA analysis. A similar table for the NMC–COLA rmse difference would show the same, except that the rmse for COLA is lower at 100 mb between the equator and 30°N. The large rmse for the COLA analysis south of 60°S probably reflects the large number of Antarctic radiosonde stations tossed by the OIQC. Lower rmse for the NMC and ECMWF analyses probably indicate these analyses accepted many of the observations rejected by the COLA analysis. Root-mean-square errors will tend to be higher at lower levels in the COLA analysis due to the tossing of observations that are below the model surface by the OIQC. Many of these observations were presumably kept in the NMC and ECMWF analyses. Root-mean-square errors computed between the station soundings and analysis geopotential heights are smaller for the NMC analyses as compared with the ECMWF analyses at some levels and some latitude bands for latitude north of 60°S.

Zonal wind rmse given in Table 4 show COLA errors to be lower than those for ECMWF almost everywhere north of 60°S. The zonal wind rmse is particularly lower in the Tropics at 500 mb and above. Root-mean-square error differences for the zonal winds over Antarctica are not as disproportionate as those for the geopotential height. The toss rate of the wind soundings was not large here, but the analysis is multivariate for winds and heights; large differences in the treatment of the height data should lead to differences in the wind analysis. Root-mean-square errors for the NMC zonal winds are generally larger than those of COLA and ECMWF. COLA rmse are larger than those for NMC south of 60°S, and ECMWF rmse are somewhat larger than NMC at midlevels in the Tropics.

d. General circulation

In this section we present two examples of striking differences in the general circulation between our reanalysis and the original ECMWF analyses for the northern winter of 1982/1983, during which the warm event was at its peak. The seasonal mean (December–February) vertically integrated moisture flux convergence in the equatorial Pacific should reflect the unusually dramatic eastward shift of precipitation that was observed during this El Niño. The results from our reanalysis (Fig. 4a) show maxima slightly south of the equator at both 170°E (over 8 mm day^{-1}) and about 155°W (over 12 mm day^{-1}). An estimate of precipitation obtained from observed outgoing longwave radiation (OLR) (Fig. 4c) shows a corresponding broad maximum that connects these maxima, although the OLR estimate is consistently higher. Precipitation is derived from the OLR from the following empirical relation based on 7 yr of data over a small region of the equatorial Pacific: precipitation (mm day^{-1}) = (25.4/30) $\times$ [63.9 − 0.22 $\times$ OLR (W m^{-2})] (P. Arkin 1985, personal communication). The even stronger satellite-derived microwave sounding unit estimate of precipitation (not shown) shows maxima that are in similar positions to those in Fig. 4a. Overall, the reanalyzed moisture flux convergence has the correct signature but is weaker than the satellite-derived precipitation by about a factor of 2. The moisture flux convergence computed from the NMC analyses (not shown) is very weak, displaying isolated maxima of only 1 mm day^{-1}. The corresponding results from the ECMWF analyses (Fig. 4b) show maxima that are also very weak in comparison to the reanalysis. The weakness of the

TABLE 3a. Root-mean-square error (rmse) computed between a thinned radiosonde dataset and COLA analyses, 0000 UTC 1 June 1982 through 1200 UTC 30 November 1983 (0000 and 1200 UTC analyses only), for geopotential heights. Units are meters.

Pressure level (mb)	rmse (m) 90°–60°S	rmse (m) 60°–30°S	rmse (m) 30°S–0°	rmse (m) 0°–30°N	rmse (m) 30°–60°N	rmse (m) 60°–90°N
100	159.0	46.9	73.6	57.1	41.3	36.4
200	153.3	37.4	40.7	28.9	30.7	26.9
300	151.1	36.8	27.3	20.2	24.1	22.3
500	149.5	29.8	16.1	13.5	14.1	13.8
700	156.2	24.5	11.7	11.6	10.0	9.6
850	172.5	24.8	11.7	13.6	12.5	9.1
1000	190.5	28.7	16.0	25.0	19.6	13.4

TABLE 3b. As in Table 3a but for the difference in rmse computed between radiosondes and ECMWF and COLA analyses. Negative values indicate the rmse was lower for the ECMWF analyses. Units are meters.

Pressure level (mb)	rmse (m) 90°–60°S	rmse (m) 60°–30°S	rmse (m) 30°S–0°	rmse (m) 0°–30°N	rmse (m) 30°–60°N	rmse (m) 60°–90°N
100	−113.1	3.0	−6.4	−2.9	8.7	8.4
200	−114.9	−0.8	4.7	4.9	6.3	5.8
300	−118.3	−9.7	5.0	4.7	4.5	4.2
500	−127.8	−13.0	3.5	3.9	3.2	2.8
700	−139.3	−11.2	1.8	2.4	2.5	2.2
850	−157.2	−12.1	0.7	0.2	1.1	1.8
1000	−173.3	−14.5	−1.6	−1.7	1.4	0.9

TABLE 3c. Number of radiosonde height observations (×1000) used in the computation of rmse in Tables 3a and 3b.

Pressure level (mb)	No. × 1000 90°–60°S	No. × 1000 60°–30°S	No. × 1000 30°S–0°	No. × 1000 0°–30°N	No. × 1000 30°–60°N	No. × 1000 60°–90°N
100	4.4	19.5	30.2	89.1	335.8	83.6
200	4.8	20.3	32.2	94.2	352.5	86.8
300	4.9	20.8	33.0	97.1	361.9	88.4
500	5.0	21.3	34.0	112.0	385.1	89.6
700	4.9	21.6	34.4	109.5	377.5	90.1
850	4.8	21.8	33.9	109.8	374.5	90.6
1000	4.7	21.4	27.4	98.7	355.0	90.6

signal in the ECMWF analyses is *not* due to the use of climatological SSTs in the original analyses, for the ECMWF analysis system started making use of current SSTs during July of 1982 (Trenberth 1992), nor is it due to excessive near-surface dryness in the ECMWF analyses, for the 1000 mb mean tropical specific humidity is in fact greater in the ECMWF analyses than in the new analyses (although the reverse is true at 850 mb) (not shown). Rather this difference is due to far stronger mean divergent circulation in the reanalyses, as witnessed by the much stronger mid-Pacific divergence at 200 mb (not shown).

TABLE 4a. Root-mean-square errors computed between a thinned radiosonde dataset and COLA analyses, 0000 UTC 1 June 1982 through 1200 UTC 30 November 1983 (0000 and 1200 UTC analyses only), for zonal wind. Units are m s^{-1}.

Pressure level (mb)	rmse (m s^{-1}) 90°–60°S	rmse (m s^{-1}) 60°–30°S	rmse (m s^{-1}) 30°S–0°	rmse (m s^{-1}) 0°–30°N	rmse (m s^{-1}) 30°–60°N	rmse (m s^{-1}) 60°–90°N
100	5.2	5.1	4.3	3.4	2.8	2.2
200	5.4	5.4	4.4	3.3	3.5	2.6
300	6.9	5.3	3.5	3.2	4.2	4.1
500	5.7	4.0	2.5	2.7	3.1	3.1
700	5.6	3.5	2.4	2.6	2.8	2.7
850	6.8	3.7	2.4	2.5	2.9	2.9
1000	5.5	4.1	2.3	2.0	2.5	3.0

TABLE 4b. As in Table 4a but for the difference in rmse computed between rawinsondes and ECMWF and COLA analyses. Negative values indicate the rmse was lower for the ECMWF analyses. Units are m s^{-1}.

Pressure level (mb)	rmse (m s^{-1}) 90°–60°S	rmse (m s^{-1}) 60°–30°S	rmse (m s^{-1}) 30°S–0°	rmse (m s^{-1}) 0°–30°N	rmse (m s^{-1}) 30°–60°N	rmse (m s^{-1}) 60°–90°N
100	–2.1	0.4	1.5	1.3	0.5	0.2
200	–1.7	0.7	1.5	1.3	0.6	0.2
300	–1.7	0.6	1.8	1.2	0.4	0.2
500	–1.4	0.2	1.3	0.8	0.4	0.2
700	–1.4	0.1	0.9	0.6	0.3	–0.1
850	–1.8	–0.3	0.5	0.3	0.1	–0.1
1000	–0.0	–0.3	0.5	0.3	0.2	–0.0

TABLE 4c. Number of rawinsonde observations (×1000) used in the computation of the rmse in Tables 4a and 4b.

Pressure level (mb)	No. × 1000 90°–60°S	No. × 1000 60°–30°S	No. × 1000 30°S–0°	No. × 1000 0°–30°N	No. × 1000 30°–60°N	No. × 1000 60°–90°N
100	4.8	22.0	41.8	92.8	316.4	78.6
200	5.7	28.9	53.4	106.5	339.8	83.2
300	5.9	31.4	58.2	115.5	357.8	85.7
500	6.1	33.4	66.3	143.4	407.3	87.7
700	5.7	34.7	75.9	166.2	416.1	87.7
850	5.7	36.0	83.9	179.6	403.5	86.6
1000	0.1	5.8	12.1	61.0	119.2	44.2

A measure of the overall strength of the divergent component of the transient circulation is afforded by the (vertically integrated) divergent transient kinetic energy. To determine the scale dependence of this quantity, we have calculated it as a function of two-dimensional wavenumber n (as in Straus and Huntley 1994), and the results are shown (along with the rotational component) in Fig. 5. While the high wavenumber (n greater than 30) differences in the divergent kinetic energy can be ascribed to discrepan-

cies in the resolution of the original datasets,[1] the very substantial difference in the peak centered at global wavenumber 8 indicates a real difference in the large-scale flow. The rotational components show little difference.

5. Summary

To assess the feasibility of retrospectively analyzing the available atmospheric observations from a past period, we have used an optimum interpolation objective analysis scheme, a complex quality control algorithm, and a state-of-the-art atmospheric general circulation model in order to reproduce the global gridded atmospheric analysis for the period May 1982 through November 1983. We have obtained all the necessary data from NCAR and from NCDC for both the atmospheric observations input streams and for the global boundary conditions. These input data included observations that were not available in real time as a result of operational forecasting time constraints. We have cycled the data assimilation and model integration codes so as to produce a global analysis every 6 h for the target period. The identical procedure was employed throughout the record in order to minimize inhomogeneities in the analysis that results from changes in quality control algorithm, optimum interpolation scheme, or first guess model integration. We have analyzed the quality control statistics of the input data streams, and we have compared the resulting retrospective analyses with the contemporaneous analyses available for that time.

We have determined that it is possible to conduct retrospective analysis of atmospheric observations, and that such a reanalysis provides a highly valuable dataset for evaluation of the global circulation. Assembling the datasets requires painstaking attention to detail, as does the evaluation of the quality control procedures. There were times when the reanalysis was run with missing data (see Table 1), when we know that data (for instance, radiosonde heights) is always available. Although the data was not present in the archive that we used, a search could probably have located the missing observations. Time did not allow us to make this search. Future reanalysis efforts could benefit from a complete data archive. Perhaps a common reanalysis database could be developed and maintained by use of all parties interested in performing reanalyses.

We feel that our reanalysis would not have been possible without the use of a flexible, interactive graphics display program. We used GrADS, which was developed here at COLA. Bad data are easy to identify using the reanalyses, the observations, and GrADS. The OIQC will remove many of these data, but per-

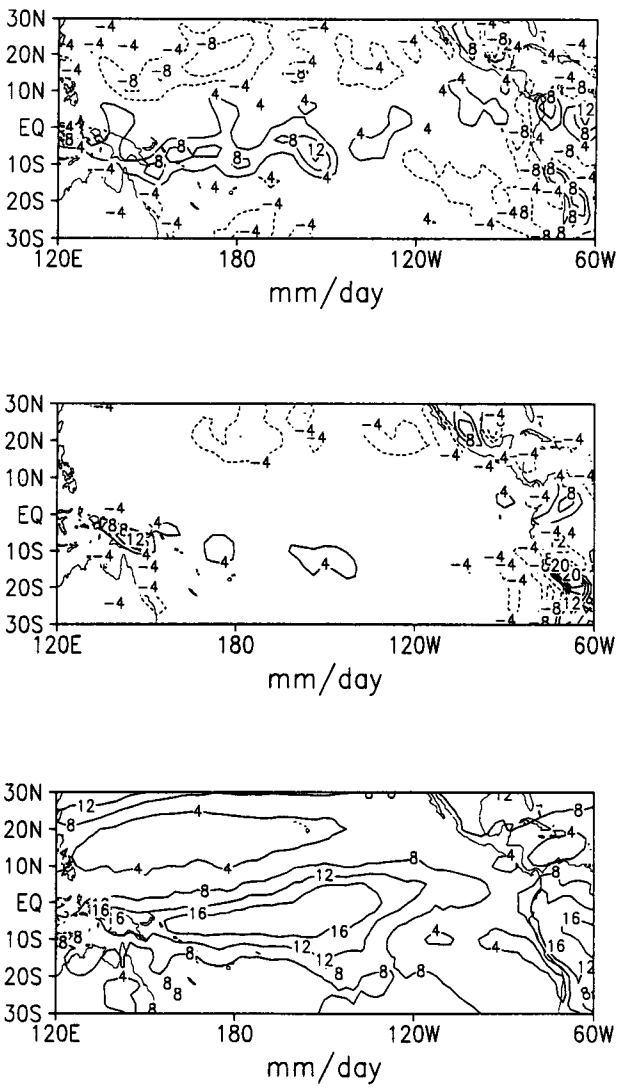

FIG. 4. Vertically integrated moisture flux convergence (a) and (b) compared with precipitation (c) for the season of December–February 1982/83 over the Pacific basin. (a) From the COLA reanalysis, contour interval of 4 mm day^{-1}. (b) From the ECMWF analyses, contour interval of 4 mm day^{-1}. (c) From outgoing longwave radiation data, contour interval of 4 mm day^{-1}. In all cases, the zero contour has been omitted.

[1]Our reanalyses were available (on pressure surfaces) in spectral coefficients, with the truncation of R40. In contrast, the ECMWF (twice-daily) analyses used were those available at NCAR on a 144 × 73 (2.5° long × 2.5° lat) grid. To make these datasets more comparable, we interpolated the ECMWF analyses onto a 96 × 80 Gaussian grid (3.75° long × ~2° lat), which is the grid appropriate for an R30 truncation. For the calculation of the divergences shown in Fig. 4, the reanalyzed coefficients were truncated to R30 before transforming to the 96 × 80 Gaussian grid. Figure 5 required transforming the ECMWF analyses into R30 spectral form.

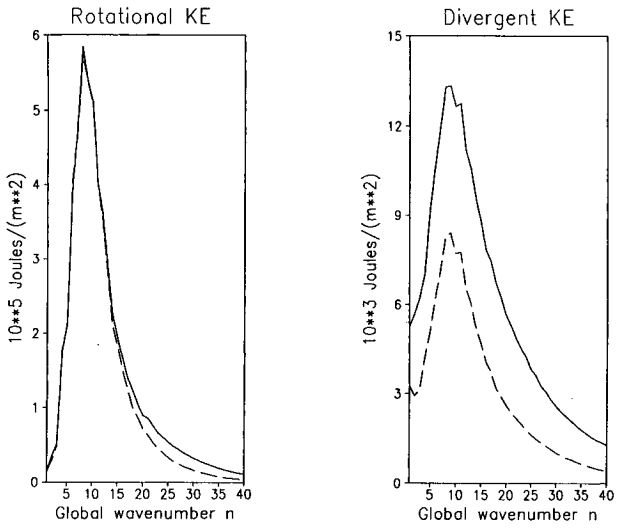

FIG. 5. Vertically integrated rotational and divergent kinetic energy as a function of global wavenumber n for the winter season of December–February 1982/83. The solid line is from the COLA reanalysis, the dashed line from ECMWF analyses. The rotational kinetic energy is in units of 10^5 J m^{-2}, while the divergent kinetic energy is in units of 10^3 J m^{-2}.

haps computational resources are now sufficient to consider removing or correcting some of these data a priori. In their reanalysis, NMC will use a system devised by Collins and Gandin (1990) to correct gross errors in radiosonde observations. Since reanalysis of multiple years of observations is a serial process that requires faster than real-time processing, automatic and manual procedures for confirming the quality of the large volume of observations and resulting analyses must be used.

We have found that our analysis was highly sensitive to the first guess model systematic error in regions where few radiosondes are available, notably south of 60°S. This was a particularly acute problem in the austral winter in the vicinity of Antarctica where the vast expanse of the Southern Ocean with its dearth of observing stations contrasts with the coastal region where several radiosonde stations were reporting. The drift toward (erroneous) model climatology over the oceanic areas during the austral winter was so large, that the coastal radiosondes were, more often than not, tossed in favor of the first guess. It is important that future reanalysis efforts consider that the various components in a model/analysis system may interact differently in different seasons, in a manner that might lead to systematic error.

Our comparison with the contemporaneous analysis shows that there are serious deficiencies in the older analyses, particularly in the divergent part of the circulation. The transient part of the divergent circulation is underestimated in the older analysis by at least a factor of 2 in tropical latitudes. Trenberth and Olson (1988a) point out that the divergent wind in the Tropics is related to intense diabatic heating from tropical convection over large areas, and that the representation of the divergent wind in the analysis will depend upon the NNMI. The use of a diabatic NNMI along with a GCM possessing advanced formulations of atmospheric radiation and moisture led to a greatly improved representation of the divergent circulation in the COLA reanalysis.

In the region of the strong El Niño event in the tropical Pacific, the 1000 mb virtual temperature reanalysis differs from the contemporaneous NMC analysis by as much as 4° in the monthly mean. The pattern of vertically integrated moisture flux convergence over the tropical Pacific Ocean was significantly closer to the pattern of rainfall (as suggested by OLR data) for the COLA reanalysis than in the ECMWF operational analysis, in spite of the fact that the latter employed the correct boundary conditions. The obvious implication is that analysis of ENSO events and other near-surface phenomena are substantially improved by the inclusion of the appropriate boundary conditions in combination with a state-of-the-art atmospheric general circulation model.

In the COLA reanalysis, we encountered a spinup problem running the COLA GCM for 6-h forecasts. Rainfall over land in tropical regions was too low, which in turn caused the soil moisture to become too dry. Future reanalysis efforts might consider whether additional observed surface conditions could be used to improve representation of the atmospheric circulation.

The serious discrepancies in our reanalysis in the extreme southern latitudes indicate that reanalysis should be undertaken in series. That is, a single retrospective analysis is inadequate and reanalysis should be contemplated as a sequence of such global analyses. Systematic errors that may arise from the interaction of the various components of the reanalysis system can be identified and remedied in a future reanalysis. Although we have only performed a single reanalysis, further reanalyses can be improved by making use of the quality control statistics from our reanalysis to determine which observations might be suitable for post facto correction, and by helping to identify those stations that might be affected by systematic error.

Acknowledgments. We wish to thank the Development Division of the National Meteorological Center for providing their Global Data Assimilation System, Jack Woollen for the use of his OIQC program, and the Data Support Section of the Scientific Computing Division at NCAR for providing the COADS data. This research was supported by the National Science Foundation and the National Oceanic and Atmospheric Administration through Grant ATM9344212.

Appendix: Data products of the COLA reanalysis

All data are available four times per day, for the period 0000 UTC 1 May 1982 through 1800 UTC 30 November 1983. The mandatory pressure levels are 1000, 850, 700, 500, 400, 300, 250, 200, 150, 100, 70, and 50 mb. Sigma levels for the COLA model are .995, .981, .960, .920, .856, .777, .688, .594, .497, .425, .375, .325, .275, .225, .175, .124, .074, and .021.

Analysis fields (on 12 mandatory pressure levels; uninitialized):

- Geopotential height (m)
- Zonal wind (m s^{-1})
- Meridional wind (m s^{-1})
- Relative humidity (%) (first six levels only)
- Virtual temperature (K)

Observations (all data streams):

- Observations rejected by OIQC
- Forecast increments (observation–first guess) for all observations accepted by OIQC

Analysis error standard deviations (on 12 mandatory pressure levels):

- Geopotential height (m)
- Relative humidity (%) (first six levels only)

First guess (on mandatory pressure levels; 6-h forecast):

- Geopotential height (m)
- Zonal wind (m s^{-1})
- Meridional wind (m s^{-1})
- Relative humidity (%)
- Virtual temperature (K)

Forecast model output (6-h forecast):

Instantaneous fields (surface)
- In surface pressure (cb)
- Roughness length (m)
- Surface temperature (K)
- Deep soil temperature (K)
- Moisture storage on canopy (m)
- Moisture storage on ground (m)
- Soil wetness of surface (fraction)
- Soil wetness of root zone (fraction)
- Soil wetness of drainage zone (fraction)

Instantaneous fields (18 sigma levels)
- Divergence (s^{-1})
- Vorticity (s^{-1})
- Specific humidity
- Virtual temperature (K)

6-h mean fields (surface)
- Surface temperature (K)
- Surface pressure (cb)
- Sensible heat flux from surface (W m^{-2})
- Latent heat flux from surface (W m^{-2})
- Surface zonal wind stress (Pa)
- Surface meridional wind stress (Pa)

6-h mean fields (18 sigma levels)
- Divergence (s^{-1})
- Vorticity (s^{-1})
- Specific humidity
- Virtual temperature (K)
- Vertical velocity (mb day^{-1})

6-h accumulated moisture fields
- Total precipitation (mm day^{-1})
- Convective precipitation (mm day^{-1})
- Runoff (mm day^{-1})
- Precipitable water (mm)
- Vertically integrated moisture flux convergence (kg m^{-2} s^{-1})

6-h mean radiation fields (one level) (in W m^{-2})
- Outgoing longwave at top
- Shortwave absorbed at ground
- Net longwave at bottom
- Downward longwave at bottom (clear)
- Outgoing longwave at top (clear)
- Downward shortwave at ground (clear)
- Upward shortwave at ground (clear)
- Upward shortwave at top (clear)
- Shortwave absorbed by earth/atmosphere (clear)
- Shortwave absorbed at ground (clear)
- Net longwave at bottom (clear)

6-h mean radiation fields (18 sigma levels) (in K s^{-1})
- Vertical diffusion heating
- Radiative heating
- Nonradiative heating

References

Bengtsson, L., and J. Shukla, 1988: Integration of space and in situ observations to study climate change. *Bull. Amer. Meteor. Soc.*, **69,** 1130–1143.

Burridge, D., 1994: Activities of the CAS/JSC working group on numerical experimentation. *Research activities in atmospheric and oceanic modelling, WMO/TD-No. 592,* iii–ix. [Available from

World Meteorological Organization, C.P. No. 2300, CH-1211, Geneva 2, Switzerland.]

Collins, W. G., and L. S. Gandin, 1990: Comprehensive hydrostatic quality control at the National Meteorological Center. *Mon. Wea. Rev.*, **118,** 2754–2767.

Dewey, K. F., and R. Heim Jr., 1982: A digital archive of Northern Hemisphere snow cover, November 1966 through December 1980. *Bull. Amer. Meteor. Soc.*, **63,** 1132–1141.

Dey, C. H., and L. L. Morone, 1985: Evolution of the National Meteorological Center Global Data Assimilation System: January 1982–December 1983. *Mon. Wea. Rev.*, **113,** 304–318.

DiMego, G. J., P. A. Phoebus, and J. E. McDonell, 1985: Data processing, quality control, and selection for optimum interpolation analysis of the National Meteorological Center. *Workshop on the Use and the Quality Control of Meteorological Observations,* Reading, U.K., ECMWF, 325–368. [Available from European Centre for Medium-Range Weather Forecasts, Shinfield Park, Reading RG2 9AX, U.K.]

Gandin, L. S., 1988: Complex quality control of meteorological observations. *Mon. Wea. Rev.*, **116,** 1137–1156.

Harshvardhan, R. Davies, D. A. Randall, and T. G. Corsetti, 1987: A fast radiation parameterization for general circulation models. *J. Geophys. Res.*, **92,** 1009–1016.

Hou, Y.-T., 1990: Cloud-Radiation-Dynamics Interaction. Ph.D. Thesis, University of Maryland, 209 pp.

Jenne, R. L., 1975: Data sets for meteorological research. NCAR Tech. Note NCAR-TN/1A-111, 194 pp. [NTIS No. PB246564.]

Kalnay, E., and Coauthors, 1993: The NMC/NCAR CDAS/Reanalysis Project. NMC Office Note 401, 42 pp.

Kidwell, K. B., 1991: *NOAA Polar Orbiter Data User's Guide.* National Climatic Data Center, Satellite Data Services Division, 206 pp. [Available from Satellite Services Division, Princeton Executive Square, Rm. 100, Washington, DC 20233.]

Kinter, J. L., III, and J. Shukla, 1989: Meeting review: Reanalysis for TOGA (Tropical Oceans–Global Atmosphere), 1–3 February 1989, Center for Ocean–Land–Atmosphere interactions. *Bull. Amer. Meteor. Soc.*, **70,** 1422–1427.

——, ——, L. Marx, and E. K. Schneider, 1988: A simulation of the winter and summer circulations with the NMC global spectral model. *J. Atmos. Sci.*, **45,** 2486–2522.

Kuo, H. L., 1965: On the formation and intensification of tropical cyclones through latent heat release by cumulus convection. *J. Atmos. Sci.*, **22,** 40–63.

Lacis, A., and J. E. Hansen, 1974: A parameterization of the absorption of solar radiation in the earth's atmosphere. *J. Atmos. Sci.*, **31,** 118–133.

Machenauer, B., 1977: On the dynamics of gravity oscillations in a shallow water model, with applications to normal mode initialization. *Beitr. Phys. Atmos.*, **50,** 253–271.

McInturff, R. M., F. G. Finger, K. W. Johnson, and J. D. Laver, 1979: Day–night differences in radiosonde observations of the stratosphere and troposphere. NOAA Tech. Memo. NWS NMC 63, 47 pp.

Mellor, G. L., and T. Yamada, 1982: Development of a turbulence closure model geophysical fluid problems. *Rev. Geophys. Space Phys.*, **20,** 851–875.

Miyakoda, K., and J. Sirutis, 1977: Comparative integrations of global models with various parameterized processes of subgrid scale vertical transport: Description of the parameterizations. *Beitr. Phys. Atmos.*, **50,** 445–487.

NMC Development Division, 1988: Research version of the medium range forecast model. NMC Documentation Series 1.

Phillips, N. A., 1957: A coordinate system having some special advantages for numerical forecasting. *J. Meteor.*, **14,** 184–185.

Reynolds, R. W., 1984: The sea surface temperatures during the 1982–1983 El Niño event. *Proc. Eighth Annual Climate Diagnostics Workshop,* Downsview, Ontario, Canada, Climate Analysis Center, NOAA, 86–91.

——, and D. C. Marsico, 1993: An improved real-time global sea surface temperature analysis. *J. Climate,* **6,** 114–119.

Sato, N., P. J. Sellers, D. A. Randall, E. K. Schneider, J. Shukla, J. L. Kinter III, Y.-T. Hou, and E. Albertazzi, 1989: Effects of implementing the simple biosphere model (SiB) in a general circulation model. *J. Atmos. Sci.*, **46,** 2757–2782.

Schubert, S. D., R. B. Rood, and J. Pfaendtner, 1993: An assimilated dataset for earth science applications. *Bull. Amer. Meteor. Soc.*, **74,** 2331–2342.

Sela, J. G., 1980: Spectral modeling at the National Meteorological Center. *Mon. Wea. Rev.*, **108,** 1279–1292.

Sellers, P. J., Y. Mintz, Y. C. Sud, and A. Dalcher, 1986: A simple biosphere model (SiB) for use with general circulation models. *J. Atmos. Sci.*, **43,** 505–531.

Slingo, J. M., 1987: The development of verification of a cloud prediction scheme for the ECMWF model. *Quart. J. Roy. Meteor. Soc.*, **13,** 899–927.

Slutz, R. J., S. J. Lubker, J. D. Hiscox, S. D. Woodruff, R. L. Jenne, D. H. Joseph, P. M. Steurer, and J. D. Elmo, 1985: *COADS: The Comprehensive Ocean-Atmosphere Data Set.* Release 1. Climate Research Program, ERL/NOAA, Boulder, CO, 39 pp. [NTIS No. PB86-105723.]

Straus, D. M., and M. A. Huntley, 1994: Interactions between moist heating and dynamics in atmospheric predictability. *J. Atmos. Sci.*, **51,** 447–464.

Tiedtke, M., 1984: The sensitivity of the time mean large scale flow to cumulus convection in the ECMWF model. *Workshop on Convection in Large Scale Numerical Models,* Reading, U.K., ECMWF, 297–316. [Available from European Centre for Medium-Range Weather Forecasts, Shinfield Park, Reading RG2 9AX, U.K.]

Trenberth, K. E., 1992: Global analyses from ECMWF and atlas of 1000 to 10 mb circulation statistics. NCAR Tech. Note NCAR/TN 373 + STR, 191 pp. [NTIS No. PB92 218718/AS.]

——, and J. G. Olson, 1988a: An evaluation and intercomparison of global analyses from the National Meteorological Center and the European Centre for Medium-Range Weather Forecasts. *Bull. Amer. Meteor. Soc.*, **69,** 1047–1057.

——, and ——, 1988b: Evaluation of NMC global analyses: 1979–1987. NCAR Tech. Note NCAR/TN-299 + STR, 82 pp. [Available from National Center for Atmospheric Research, P.O. Box 3000, Boulder, CO 80307-3000.]

Walton, C., 1985: Satellite measurement of sea surface temperature in the presence of volcanic aerosols. *J. Climate Appl. Meteor.*, **24,** 501–507.

Woollen, J. S., 1991: New NMC operational OI quality control. Preprints, *Ninth Conf. on Numerical Prediction,* Denver, CO, Amer. Meteor. Soc., 24–27.

Xue, Y., P. J. Sellers, J. L. Kinter III, and J. Shukla, 1991: A simplified biosphere model for global climate studies. *J. Climate,* **4,** 345–364.